EXTENDED PDF FORMAT
SPONSORED BY

BIO-RAD

http://discover.bio-rad.com



An Early Cretaceous Tribosphenic Mammal and Metatherian Evolution

Zhe-Xi Luo, *et al.*

Science **302**, 1934 (2003);
DOI: 10.1126/science.1090718

The following resources related to this article are available online at www.sciencemag.org (this information is current as of January 2, 2007):

Updated information and services, including high-resolution figures, can be found in the online version of this article at:
http://www.sciencemag.org/cgi/content/full/302/5652/1934

Supporting Online Material can be found at:
http://www.sciencemag.org/cgi/content/full/302/5652/1934/DC1

A list of selected additional articles on the Science Web sites **related to this article** can be found at:
http://www.sciencemag.org/cgi/content/full/302/5652/1934#related-content

This article **cites 12 articles**, 1 of which can be accessed for free:
http://www.sciencemag.org/cgi/content/full/302/5652/1934#otherarticles

This article has been **cited by** 35 article(s) on the ISI Web of Science.

This article has been **cited by** 8 articles hosted by HighWire Press; see:
http://www.sciencemag.org/cgi/content/full/302/5652/1934#otherarticles

This article appears in the following **subject collections**:
Paleontology
http://www.sciencemag.org/cgi/collection/paleo

Information about obtaining **reprints** of this article or about obtaining **permission to reproduce this article** in whole or in part can be found at:
http://www.sciencemag.org/help/about/permissions.dtl

Downloaded from www.sciencemag.org on January 2, 2007

Science (print ISSN 0036-8075; online ISSN 1095-9203) is published weekly, except the last week in December, by the American Association for the Advancement of Science, 1200 New York Avenue NW, Washington, DC 20005. Copyright c 2006 by the American Association for the Advancement of Science; all rights reserved. The title SCIENCE is a registered trademark of AAAS.

21. Despite the absence of key information about sediment caliber, stream load, original gradients, and original basin morphometry that would be needed to perform a quantitative assessment of the hydrology of the Holden NE basin, it is somewhat informative to examine those aspects of the system for which some reasonable assumptions can be made. The relatively low gradient (0.35°) of the well-exposed meander zone seen in Fig. 2A, and the measurement of a typical channel width of 50 m, permits the calculation of flow velocity using the Manning equation with appropriately gravity-modified parameters (*33*) if one assumes a range of possible flow depths and Manning roughness coefficients. For values of roughness corresponding to 0.04 on Earth (a bed mostly of fine-grained materials but with some stones), flow depths of a few meters on Mars would flow at a few meters per second, producing discharges of a few hundred cubic meters per second. Terrestrial field experience suggests that this rate is consistent with the size and configuration of the meanders seen (although perhaps on the high end of such an estimate). Were this discharge to occur today, it would fill the existing, eroded floor of Holden NE Crater to the –1300 m level (the level at which both major valleys entering the crater lose definition) in roughly 20 years. Although fraught with uncertainties owing to dependencies on climate, catchment basin size and geometry, and lake volume, the Holden NE values fall within a range that includes comparable desert environment lakes such as the Great Salt Lake in Utah and the Sea of Galilee (inflow rates of tens to hundreds of cubic meters per second, lake volumes of 10^9 to 10^{11} m^3, and filling times of decades). These calculations simply show that the relations are internally consistent with similar relations seen on Earth, not necessarily that the situations are identical.
22. As part of our study, we targeted 158 locations identified by previous investigations [e.g., appendix B in (*34*)] as potential "alluvial fans" and "deltas" (*34, 35*) and more than 100 additional locations exhibiting similar topographic relations (valleys entering depressions). As of October 2003, some 200 MOC images covering approximately 80 locations had been acquired and inspected. All of these images show features quite different from those discussed in this work, generally falling into two categories. The most prevalent category is one in which the floors of the valley and crater are concordant, showing no discernible expression of deposition (e.g., MOC images E04-01284, E23-01302, and R02-00995). In these cases, alluvial deposits may exist but have been buried by some process that filled the crater, or may have once existed but have since been completely stripped away. In a relatively small number of cases (the second category), a discernible apron of material is seen at the point where the valley enters the crater. Although the aprons have some attributes of alluvial fans (they are conical in three-dimensional form, have longitudinal slopes ≥2° and convex transverse sections, and occur adjacent to high-standing relief), they have three characteristics that distinguish them from the fan described in this work: They consist of a single (rather than multiple) lobe of material, they lack a radial (or distributary) pattern of conduits, and they display concentric steps in their surface's descent to the crater floor (e.g., MOC images E02-00508 and R02-00093). The concentric steps are unique to the aprons, as the adjacent crater walls do not display such forms (that is, the steps are not wave-cut terraces). In some cases, the volume of the apron appears to be equal to the volume of the valley (e.g., MOC images E05-02330, E09-00340, and E11-00948). These aprons appear to be the result of mass movements rather than fluvial processes, with the concentric steps resulting from successive surges of the material as it moved out of the valley or, more likely, as the expression of compressive stress in the material as it came to rest within the crater.
23. We use the term "rhythmically layered" to denote a sequence of tens to hundreds of repeated layers (or packages of layers too fine to resolve in MOC images) of essentially identical thickness and outcrop expression.
24. M. C. Malin, K. S. Edgett, *Science* **290**, 1927 (2000).
25. W. E. Galloway, in *Deltas, Models for Exploration*, M. L. Broussard, Ed. (Houston Geological Society, Houston, TX, 1975), pp. 87–98.
26. W. Nemec, in *Coarse-Grained Deltas,* A. Colella, D. B. Prior, Eds., *Intl. Assn. Sedimentol. Spec. Pub. 10,* 3 (1990).
27. T. C. Blair, J. G. McPherson, *J. Sediment. Res. A* **64**, 450 (1994).
28. GMT—The Generic Mapping Tools (http://gmt.soest.hawaii.edu).
29. P. Wessel, W. H. F. Smith, *Eos* **72**, 441 (1991).
30. R. P. Miller, *J. Geol.* **45**, 432 (1937).
31. J. Maizels, *Palaeogeogr. Palaeoclimatol. Palaeoecol.* **76**, 241 (1990).
32. Mars Channel Working Group, *Geol. Soc. Am. Bull.* **94**, 1035 (1983).
33. P. Komar, *Icarus* **37**, 156 (1979).
34. N. A. Cabrol, E. A. Grin, *Icarus* **149**, 291 (2001).
35. G. G. Ori, L. Marinangeli, A. Baliva, *J. Geophys. Res.* **105**, 17629 (2000).
36. We thank R. A. MacRae for stimulating discussions, and R. M. E. Williams and V. R. Baker for their perceptive and insightful comments and suggestions that were instrumental in refining and focusing this paper. We acknowledge the contribution to this work made by the MGS/MOC and Mars Odyssey/THEMIS operations teams at Malin Space Science Systems, Arizona State University, the Jet Propulsion Laboratory (JPL), and Lockheed Martin Astronautics. Supported by JPL contract 959060 and Arizona State University contract 01-081 (under JPL contract 1228404 and NASA prime contract task 10079).

18 August 2003; accepted 28 October 2003
Published online 13 November 2003;
10.1126/science.1090544
Include this information when citing this paper.

Downloaded from www.sciencemag.org on January 2, 2007

An Early Cretaceous Tribosphenic Mammal and Metatherian Evolution

Zhe-Xi Luo,[1,2]* Qiang Ji,[2,3] John R. Wible,[1] Chong-Xi Yuan[4]

Derived features of a new boreosphenidan mammal from the Lower Cretaceous Yixian Formation of China suggest that it has a closer relationship to metatherians (including extant marsupials) than to eutherians (including extant placentals). This fossil dates to 125 million years ago and extends the record of marsupial relatives with skeletal remains by 50 million years. It also has many foot structures known only from climbing and tree-living extant mammals, suggesting that early crown therians exploited diverse niches. New data from this fossil support the view that Asia was likely the center for the diversification of the earliest metatherians and eutherians during the Early Cretaceous.

Marsupials are one of the three main lineages of extant mammals (Monotremata, Marsupialia, and Placentalia) (*1, 2*). Extant marsupials, such as the opossum, kangaroo, and koala, are a subgroup of the Metatheria, which also includes all extinct mammals that are more closely related to extant marsupials than to extant placentals (*3*). Both metatherians and eutherians (including extant placentals) are subgroups of the northern tribosphenic mammal clade or Boreosphenida (*2, 4, 5*). Here we report a new boreosphenidan mammal with close affinities to metatherians, and discuss its implications for the phylogenetic, biogeographic, and locomotory evolution of the earliest eutherians and metatherians.

Sinodelphys szalayi (*6*) gen. et sp. nov. is distinguishable from all mammals (*7–11*) previously known from the Yixian Formation [125 million years ago (Ma) (*12*)] by a long list of apomorphies (*13, 14*). Numerous dental and skeletal apomorphies also distinguish *Sinodelphys* from all Cretaceous eutherians (including *Eomaia* from the Yixian Formation) (*2, 10, 15–18*). *Sinodelphys* is also more derived than the stem boreosphenidans (*4*) outside the therian crown group (metatherians + eutherians) in several dental apomorphies, but is less advanced than other metatherians including *Deltatheridium* (*3*) in dental formula (*13, 14*). Hairs are preserved as carbonized filaments and impressions around the torso of the holotype (Fig. 1). The pelage appears to have both guard hairs and denser underhairs close to the body surface.

Description and comparison. *Sinodelphys szalayi* is more closely related to extant marsupials than to extant placentals and stem taxa of boreosphenidans in its many marsupial-like apomorphies in the skeleton and anterior dentition (Fig. 1). The posterior upper incisors (I3, I4) are mediolaterally compressed with an asymmetrical, lanceolate (nearly diamond) outline in lateral view. This feature is characteristic of "didelphid-like" marsupials and the stem metatherians for which incisors are known (*19–24*), but it is absent in all known Cretaceous eutherians and mammals outside crown Theria (*7, 10, 25–27*). The first upper premolar (P1) is procumbent and close to the upper canine, fol-

[1]Carnegie Museum of Natural History, Pittsburgh, PA 15213, USA. [2]Department of Earth Science, Nanjing University, Nanjing 200017, China. [3]Chinese Academy of Geological Sciences, Beijing 100037, China. [4]China University of Geosciences, Beijing 100083, China.

*To whom correspondence should be addressed. E-mail: luoz@carnegiemuseums.org

lowed by a large diastema behind (Fig. 1C), a derived feature of Late Cretaceous metatherians and Cenozoic "didelphid-like" marsupials (*3, 19–23*). *Sinodelphys* has a mixture of derived and primitive characters in the molars. Its lower molars have developed an approximation of the entoconid to the hypoconulid [only exposed on m1 (*14*)], as in the metatherians *Asiatherium* (*28*), *Kokopellia* (*29*), and *Marsasia* (*30*). In this feature *Sinodelphys* is more marsupial-like than the stem boreosphenidans (*4, 5*) and some deltatheroidans (*3, 30–33*), in which the entoconid is indistinct or absent. However, *Sinodelphys* and the aforementioned metatherians lack the full twinning of these cusps seen in Late Cretaceous metatherians (*34*). The seven lower postcanine loci of *Sinodelphys* are present in some Late Cretaceous eutherians. The four upper molars are also present in the stem boreosphenidan *Kielantherium*, outside the basal metatherians (*3*). *Sinodelphys* lacks the inflected mandibular angular process of the more derived metatherians (*35*).

The wrist and ankle of *Sinodelphys* have many marsupial-like apomorphies (Figs. 2 and 3). In the manus of *Sinodelphys*, the carpals have a hypertrophied hamate (relative to the capitate and trapezoid), an enlarged triquetrum (relative to the lunate and distal ulna), and an enlarged scaphoid (relative to the lunate and/or trapezium). These features are characteristic of *Asiatherium* (*28*) and other metatherians (*18, 22*) and are correlated with better capacity for gripping in didelphids. By contrast, these bones are not enlarged in Cretaceous eutherians (*10, 36*) and stem mammals outside the crown Theria (*7, 8, 11*). The trapezium is large and oblong in eutherians (*10, 36*), but small and bean-shaped in *Sinodelphys* and metatherians (Fig. 2).

Sinodelphys is distinctive from all Cretaceous eutherians but similar to metatherians in many derived pedal characters. The tarsals have a transversely broad but anteroposteriorly short navicular (Fig. 2). The navicular facet on the astragalar head is spread medially along the length of the neck, such that the head with its navicular facet is asymmetrical with regard to the main axis of the astragalar neck (Fig. 3), as is typical of Cretaceous metatherians (*18*). In contrast, the navicular of Cretaceous and some Tertiary eutherians is transversely narrow and anteroposteriorly elongate, with the navicular facet restricted anteriorly on the astragalar head (Figs. 2 and 3). In some (although not all) Tertiary eutherians with a nearly hemispherical astragalar head, the navicular facet is spread to both the medial and lateral sides of the neck, so that the head is symmetrical with regard to the axis of the neck (*10, 18, 36, 37*).

Sinodelphys and metatherians also share several derived calcaneal features (Fig. 3). The calcaneocuboid facet is obliquely oriented with respect to the length of the calcaneus, and is buttressed by a large anteroventral tubercle. This is related to the habitual inversion of the distal part of the pes (*18, 38*). The base of the peroneal process is level with the cuboid facet [as in *Sinodelphys* and Paleocene metatherians (*21*)] or anterior to it [as in

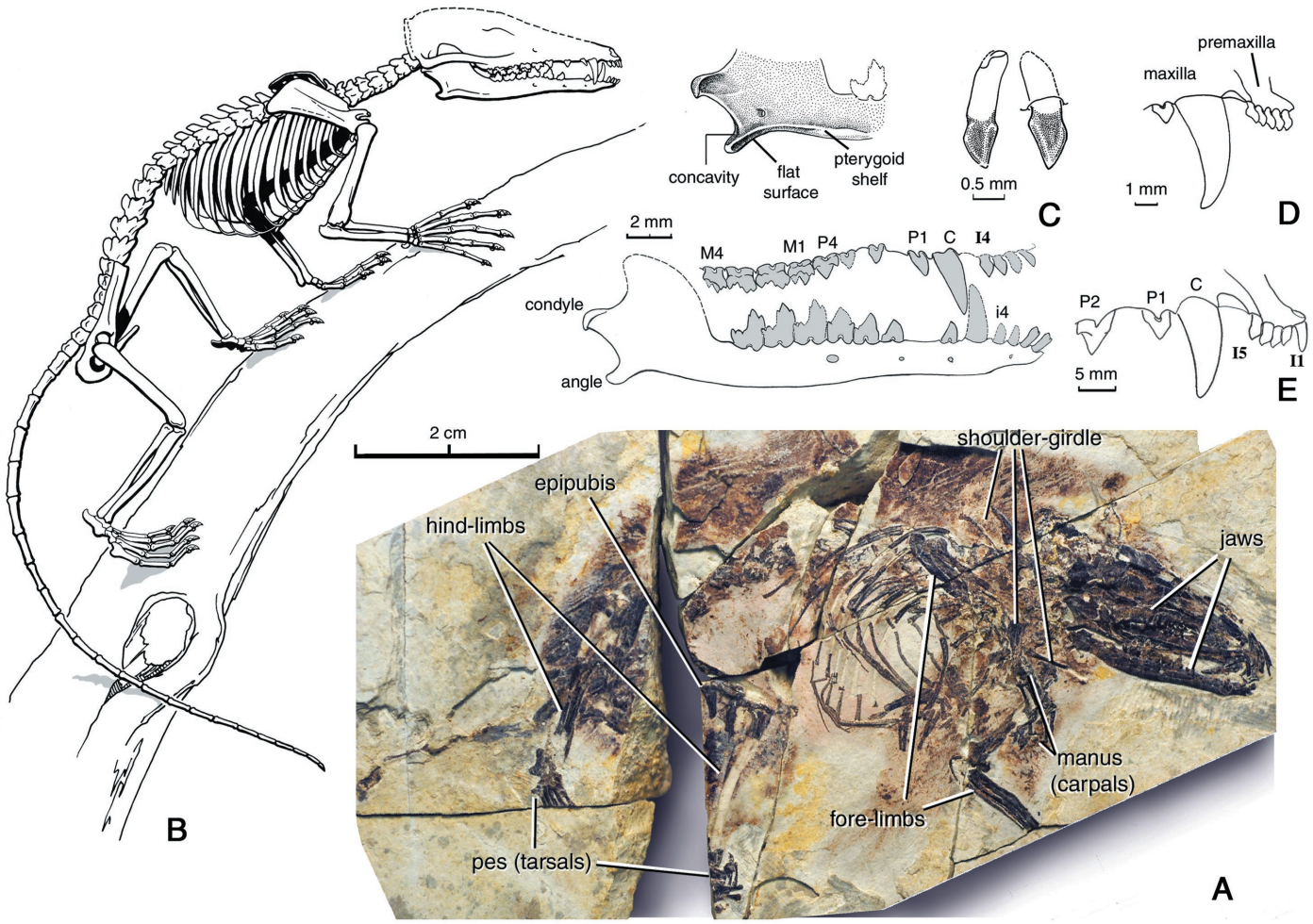


Fig. 1. *Sinodelphys szalayi* gen. et sp. nov. (**A**) Holotype (Chinese Academy of Geological Sciences CAGS00-IG03) as preserved (see also figs. S1 and S2). (**B**) Restoration of *S. szalayi* as an agile, climbing animal, active on uneven substrates and branch-walking. (**C**) Mandible, upper and lower dentitions, and medial and lateral views of I4. (**D** and **E**) Comparison of anterior dentitions of (D) the metatherian *Pucadelphys* [after (*19*)] and (E) the marsupial *Didelphis*. Dental formula for *S. szalayi*: C and c, upper (1) and lower (1) canine; I and i, upper (4) and lower (4) incisors; M and m, upper (4) and lower (3) molars; P and p, upper (4) and lower (4) premolars.

Downloaded from www.sciencemag.org on January 2, 2007

Late Cretaceous metatherians (*18*)]; the sustentacular process forms a pointed triangle. By contrast, all Cretaceous eutherians show an anteriorly oriented calcaneocuboid facet without a well-defined anteroventral tubercle; the ventral surface posterior to the calcaneocuboid facet is flat or slightly grooved in the anterior part of the calcaneus (*37*), and the base of the peroneal process is offset posteriorly from the cuboid facet. These eutherian features are primitive because they are present in stem therians outside the eutherian-metatherian clade, such as *Vincelestes* (*27*) and *Zhangheotherium* (Fig. 3H). In Cretaceous eutherians, the sustentacular process is shelf-like in ventral view, not a pointed angle as in *Sinodelphys* and metatherians (Fig. 3). *Sinodelphys* also has a much wider supraspinous fossa than infraspinous fossa at midlength of the scapula; the cranial border of the scapula has a strongly sigmoidal profile, ending anteriorly in a pronounced supraspinous incisure. The ectepicondylar region of the humerus has a shelf-like supinator crest with a sigmoidal profile. These forelimb features are well-documented, derived features of Paleocene metatherians (*19–21, 38, 39*), but are absent in Cretaceous eutherians (*10, 25, 36, 37*). Overall, *Sinodelphys* has many derived, marsupial-like features of the skeleton and anterior dentition, but its molars and mandible have a mosaic of derived metatherian features and plesiomorphies shared by eutherians and taxa outside the crown Theria.

Relationships and paleobiogeography. We estimated phylogenetic relationships of *Sinodelphys* by parsimony analysis of 380 dental, mandibular, cranial, and postcranial characters of 84 clades that range from advanced nonmammalian cynodonts to the representatives of modern marsupial orders (*14*). This data set includes the morphological features preserved in *Sinodelphys*, as well as characters known to be informative about the relationships of crown therians (*3–5, 25–27*) or shown to be useful for estimates of extant marsupial phylogenies (*18–24*). To ensure that our interpretation of metatherian relationships would not be adversely affected by undersampling of successive outgroups, our analysis also included a wide range of eutherians, stem boreosphenidans, and all other Mesozoic mammal clades (*4, 5, 40*). The phylogenetic hypotheses of *Sinodelphys*, as proposed here, are fully consistent with previously established phylogenies of all mammalian clades on the basis of global parsimony of available morphological evidence [e.g., (*4, 5, 10*)].

In our analysis, *Sinodelphys* is more closely related to marsupials than to placentals. Within metatherians, *Sinodelphys* is placed in the root of the metatherian family tree (Fig. 4A, node 4) with *Holoclemensia*, a dental taxon that has also been hypothesized to be a basal metatherian (*3*), but more plesiomorphous than *Deltatheridium*, which is placed on the next node toward crown marsupials (Fig. 4A, node 5). Metatherians from the early Late Cretaceous (Coniacian) of Uzbekistan (*30*) and *Kokopellia* (~100 Ma) from North America (*29*) are resolved into successively more derived clades toward the monophyletic group of primarily Late Cretaceous metatherians of North America (*34*),

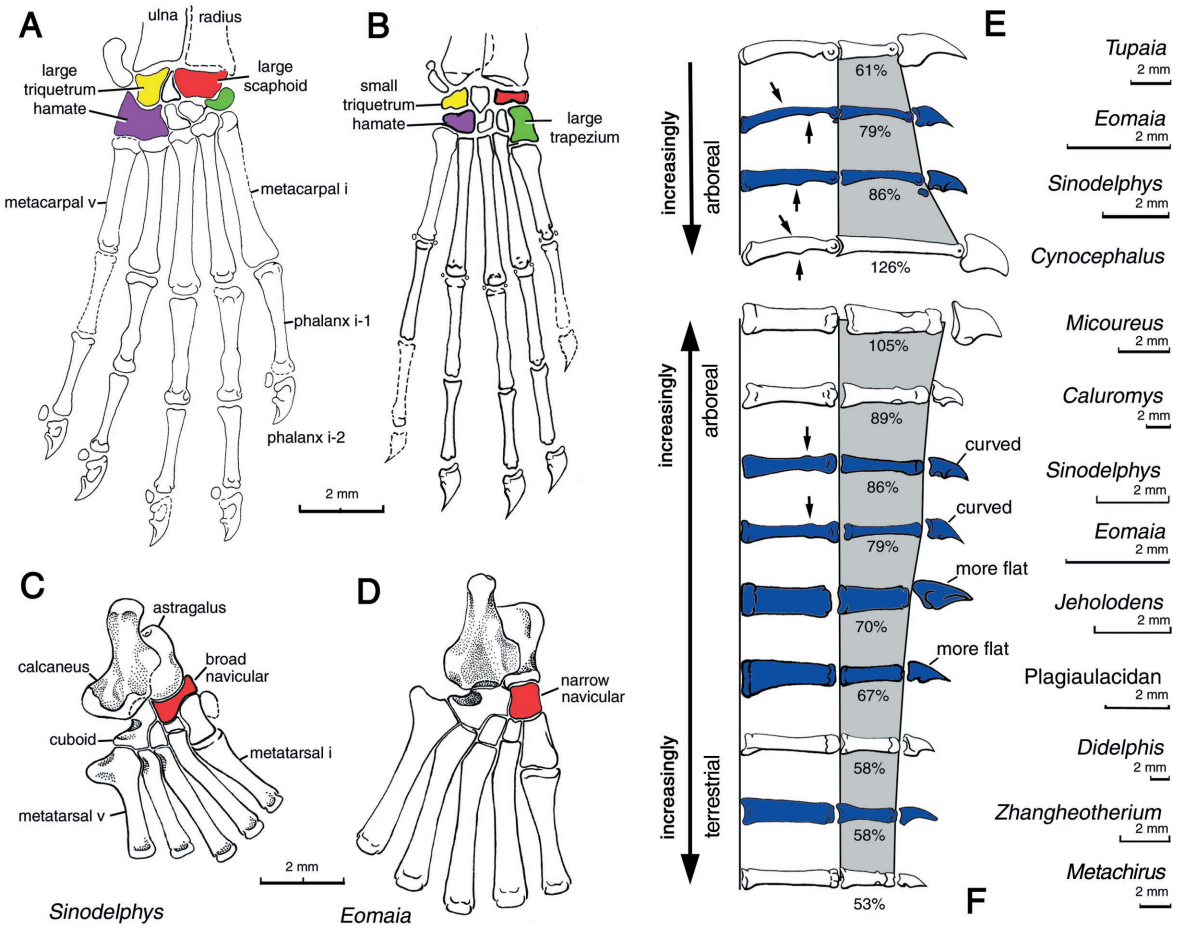


Fig. 2. Comparison of foot structure of *Sinodelphys*. (**A**) Forefoot and (**C**) hindfoot (tarsals and metatarsals) of the metatherian *Sinodelphys*; (**B**) forefoot and (**D**) hindfoot of the eutherian *Eomaia* (composite reconstruction; left side in ventral view, claws in lateral view, all to the same scale). Carpal apomorphies of metatherians (including *Sinodelphys*) (*18, 22, 28*) are listed in (*14*). See Fig. 3 for additional tarsal apomorphies of metatherians and eutherians. (**E** and **F**) Comparison of manual phalanges between the mammals of the Yixian community and (E) some modern placentals [digit 3 in lateral view after (*47*)] and (F) didelphid marsupials [digit 3, proximal and intermediate phalanges in ventral view, claws in lateral view, after (*38*)] with diverse locomotory adaptations: tree shrew *Tupaia* [scansorial, after (*47*)]; eutherian *Eomaia* (inferred to be scansorial); *Sinodelphys* (inferred to be scansorial or arboreal); flying lemur *Cynocephalus* (fully arboreal); didelphid *Micoureus* (fully arboreal); didelphid *Caluromys* (fully arboreal); the Yixian eutriconodont *Jeholodens* (inferred to be terrestrial); the Yixian multituberculate (inferred to be terrestrial); didelphid *Didelphis* (scansorial); the Yixian trechnotherian *Zhangheotherium* (inferred to be terrestrial); didelphid *Metachirus* (fully terrestrial). The proximal phalanges are standardized to the same length; percentage represents the length ratio of the intermediate to the proximal phalanges; scale varies among taxa. Arrows indicate phalangeal curvature and protuberances for digital flexor tendon sheath, typical of scansorial or arboreal mammals.

Downloaded from www.sciencemag.org on January 2, 2007

plus the Paleocene South American taxa that are proximal stem taxa to the crown marsupial clade. Because of the incompleteness of some North American Late Cretaceous taxa and character conflicts in some South American Paleocene taxa, the relationships among North and South American metatherians are not fully resolved in the strict consensus tree, a more conservative estimate of phylogeny (Fig. 4A). Nonetheless, a more relaxed estimate by the Adams consensus tree from our analysis (Fig. 4B) suggests that the South American *Pucadelphys* (*19*) and *Andinodelphys* (*24*) are close to the root of the marsupial crown clade, consistent with previous studies of these groups (*3, 24*).

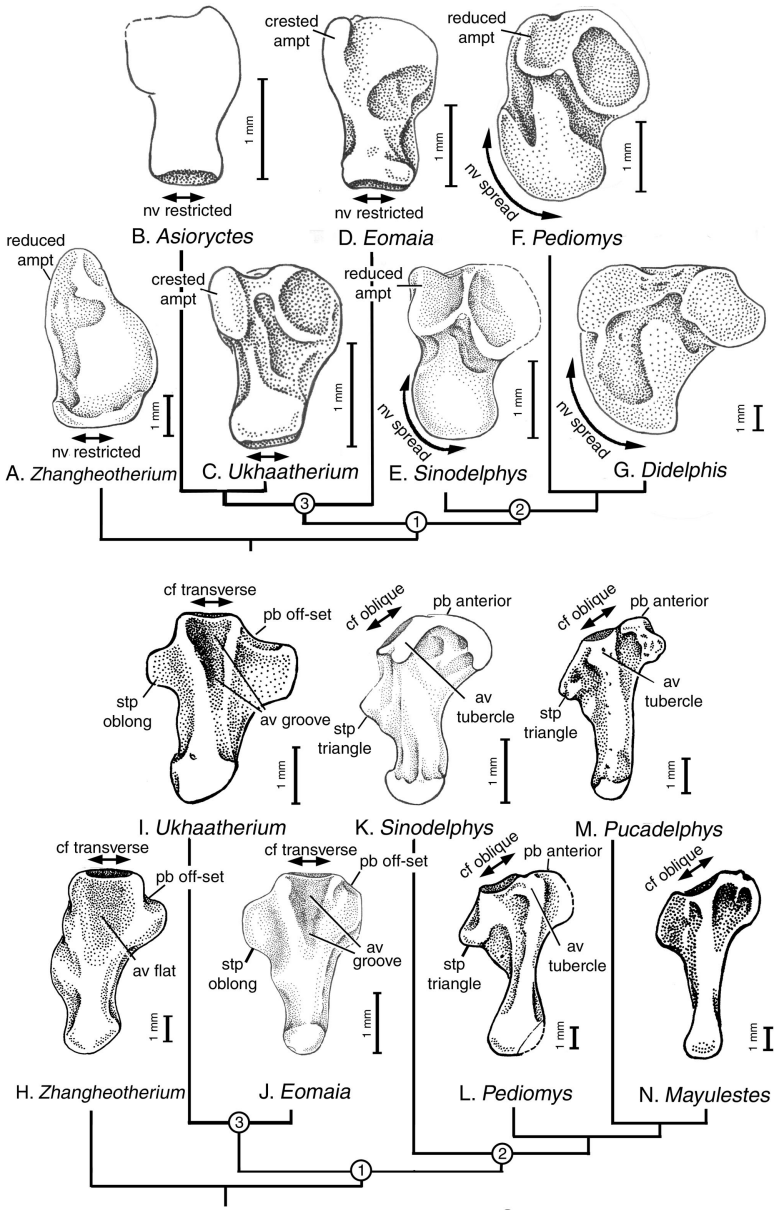


Fig. 3. Tarsal apomorphies for metatherians and eutherians. (**A** to **G**) Astragali; (**H** to **N**) calcanei (left side in ventral or plantar view unless noted otherwise; scale varies among taxa). (A) Trechnotherian *Zhangheotherium* (left, dorsal view, National Geological Museum of China NGMC 354). (B) Eutherian *Asioryctes* [outline after (*36*)]. (C) Eutherian *Ukhaatherium* [after (*37*)]. (D) Eutherian *Eomaia* (composite reconstruction). (E) Metatherian *Sinodelphys* (reconstruction from two incomplete astragali, ventral view). (F) Metatherian *Pediomys* [after (*18*)]. (G) Marsupial *Didelphis*. (H) *Zhangheotherium* (NGMC 354). (I) *Ukhaatherium* [after (*38*)]. (J) *Eomaia*. (K) *Sinodelphys* (holotype). (L) *Pediomys* [after (*18*)]. (M) Metatherian *Pucadelphys* [after (*21*)]. (N) Metatherian *Mayulestes* [after (*21*)]. Tarsal characteristics by phylogenetic nodes 1 to 3 listed in (*14*). Abbreviations: ampt, astragalar medial plantar tubercle; av, anteroventral structure (calcaneus) (flat or grooved in most nonmetatherians, tubercle in metatherians); cf, calcaneocuboid facet (transverse in nonmetatherians, oblique in metatherians); nv, navicular facet of astragalus (anteriorly restricted in most nonmetatherians, medially spread in metatherians); pb, base for peroneal process (calcaneus) (offset from anterior end of calcaneus in nonmetatherians, anteriorly placed in metatherians); stp, sustentacular process (calcaneus).

The classic views on early mammalian biogeographic evolution hold that both eutherians and metatherians originated on the northern continents [(*41*), but see (*40*)] and that early geographic evolution of metatherians proceeded from Asia and North America to North and South America, and then to South America and Australia (*18, 24*). These views are corroborated by discoveries of *Sinodelphys* (*14*) and other new eutherians and metatherians (*3, 10, 24–26, 30*). In the context of our phylogeny (Fig. 4A), the metatherian fossil record suggests the following sequence for the major episodes of diversification: divergence of metatherians and eutherians in Asia no later than 125 Ma in the Early Cretaceous (Fig. 4A, nodes 2, 3, and 4; Fig. 4B), followed by the evolution of deltatheroidan-like taxa in both Asia and North America during the late Early Cretaceous (120 to 100 Ma) (Fig. 4B), before a major metatherian diversification in North America in the Late Cretaceous (100 to 65 Ma) (Fig. 4A, nodes 6 and 7), and then the Paleocene diversification of proximal relatives to crown marsupials in South America (Fig. 4A, node 8).

Implications for morphological evolution. Marsupials and placentals make up 99.9% of all extant mammals. The phyletic divergence of metatherians from eutherians led to the different specializations in life histories (*42, 43*) and skeletal structures (*18, 38*) of extant marsupials and placentals. *Eomaia*, the earliest known member of the eutherian-placental lineage, lived around 125 Ma (*10*); thus, the marsupial-placental split must have occurred no later than this time. Recent molecular studies estimate that the marsupial orders may have diverged as early as 79 to 86 Ma (*44*). The previously oldest and uncontested metatherian [*Kokopellia* (*29*)] is ~100 Ma, with a possible deltatheroidan [*Atokatheridium* (*31*)] and *Holoclemensia* (*3*) known from 110 to 105 Ma. The previously earliest metatherian skeletal fossil is from ~75 Ma [*Asiatherium* (*28*)]. Precious little is known about the skeletal anatomy of the earliest metatherians for their first 50 million years of history before the record of *Asiatherium*.

Metatherians were previously diagnosed by the presence of three premolars and four molars (seven postcanine loci) with a single replacement at the ultimate premolar, as well as the twinning of the entoconid and hypoconulid (*34*) and the labial postcingulid (*29*) in molars. The diagnostic mandibular characters are an inflected angular process and the posterior shelf of the masseteric fossa [e.g., (*3, 14, 19, 21, 35*)]. These characteristics are supplemented by additional carpal apomorphies (such as hypertrophied hamate, triquetrum, and scaphoid) and tarsal apomorphies (such as enlargement of the navicular and the medial spread of the navicular facet on the astragalar head, as well as an oblique,

Downloaded from www.sciencemag.org on January 2, 2007

strengthened calcaneocuboid contact in a mobile transtarsal joint) (*18, 45*). *Sinodelphys* provides new information for the sequence of evolutionary acquisition of the diagnostic metatherian characters, helps fill the gaps in our knowledge of the crucial anatomical transformations that occurred in the marsupial-placental split, and helps establish the ancestral anatomy from which the derived marsupials evolved. Our phylogeny (Fig. 4A) suggests that the foremost phylogenetic distinctions between marsupials and placentals are in the anatomy of the wrist and ankle (Figs. 2 and 3). The carpal and tarsal climbing specializations were acquired first in the

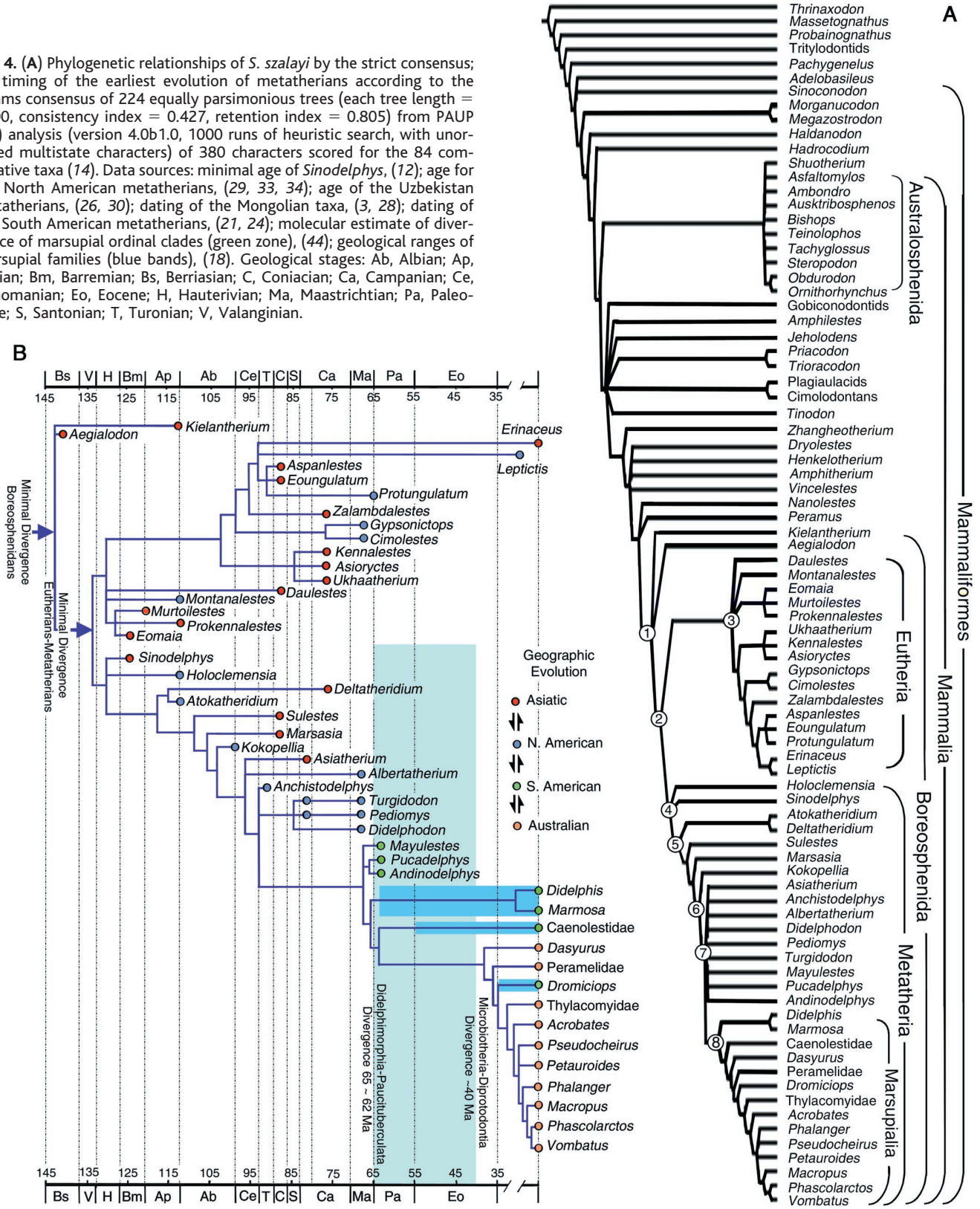


Fig. 4. (**A**) Phylogenetic relationships of *S. szalayi* by the strict consensus; (**B**) timing of the earliest evolution of metatherians according to the Adams consensus of 224 equally parsimonious trees (each tree length = 1700, consistency index = 0.427, retention index = 0.805) from PAUP (*49*) analysis (version 4.0b1.0, 1000 runs of heuristic search, with unordered multistate characters) of 380 characters scored for the 84 comparative taxa (*14*). Data sources: minimal age of *Sinodelphys*, (*12*); age for the North American metatherians, (*29, 33, 34*); age of the Uzbekistan metatherians, (*26, 30*); dating of the Mongolian taxa, (*3, 28*); dating of the South American metatherians, (*21, 24*); molecular estimate of divergence of marsupial ordinal clades (green zone), (*44*); geological ranges of marsupial families (blue bands), (*18*). Geological stages: Ab, Albian; Ap, Aptian; Bm, Barremian; Bs, Berriasian; C, Coniacian; Ca, Campanian; Ce, Cenomanian; Eo, Eocene; H, Hauterivian; Ma, Maastrichtian; Pa, Paleocene; S, Santonian; T, Turonian; V, Valanginian.

Downloaded from www.sciencemag.org on January 2, 2007

Early Cretaceous member(s) of the metatherian lineage (Fig. 4A, node 4), followed by acquisition of such marsupial dental apomorphies as the twinned entoconid and hypoconulid and labial postcingulid of the lower molars typical of Late Cretaceous metatherians (*29, 34*) and the reduced dental replacement related to specialized marsupial life history (Fig. 4A, node 7) (*46*). Characters of *Sinodelphys* also suggest that it may be possible for additional stem boreosphenidans of the Cretaceous to be sorted into the marsupial or placental lineages when the more definitive apomorphies of their anterior dentition, carpals, and tarsals become known from better fossils, even if their molars lack either placental-like or marsupial-like specializations (*33*).

The skeletal adaptations of *Sinodelphys* for climbing suggest that scansorial and arboreal adaptations of didelphid marsupials have a very ancient evolutionary origin (*18, 21, 38, 39, 45*). The forefoot of *Sinodelphys* (Fig. 2) bears resemblance to those of extant arboreal mammals (*38, 45*) in many grasping features. In phalangeal features, *Sinodelphys* is more similar to fully arboreal mammals, such as the didelphid *Caluromys* and the flying lemur *Cynocephalus*, than to scansorial taxa such as the opossum and tree shrew. The proximal manual phalanx is slightly arched dorsally (Fig. 2). Some phalanges have two protuberances for the fibrous tendon sheaths of the flexor digitorum. Distal ends of the metacarpals and phalanges are robust and trochleated. A large sesamoid bone is present at the distal phalangeal joint for all manual digits (Fig. 2). These indicate that the forefoot of *Sinodelphys* had a strong capacity to flex the digits, possibly for grasping. As in scansorial didelphids, *Sinodelphys* has a wide navicular and an expanded navicular facet on the medial side of the astragalar head, both of which are associated with an effective grasping of the medial pedal digit(s) in modern didelphids and with a wider range of inversion-eversion of the distal pedal bones at the transtarsal joint (*18, 45*). One peculiar feature of *Sinodelphys* is that its forefoot is larger (>120% in combined metapodial and phalangeal length) than the hindfoot, whereas in the contemporary eutherian *Eomaia* the forefeet and hindfeet are about the same size (Fig. 2).

The length of proximal and intermediate phalanges differs among terrestrial, scansorial, and fully arboreal didelphid marsupials (*38*) and in placental carnivorans and euarchontans (*47*). The phalangeal ratio of *Sinodelphys* (Fig. 2, E and F) is intermediate between those of fully arboreal and scansorial didelphids and is far greater than that of the fully terrestrial didelphid *Metachirus* (*38*). The intermediate phalanx in *Sinodelphys* is also more elongate than in the scansorial tree shrew. Both the manual and pedal claws in *Sinodelphys* lack the thickened dorsal rim seen in eutriconodonts, multituberculates, and stem therian mammals from the same fauna, indicating that these claws are laterally compressed, as in extant mammals capable of climbing. These convergent skeletal features for climbing of unrelated scansorial and arboreal mammals (*10, 38, 45, 47*) strongly suggest that *Sinodelphys* was an agile, scansorial mammal capable of grasping and branch-walking, and active both on the ground and in trees or shrubs (e.g., like the scansorial opossum *Didelphis* or tree-living *Caluromys*).

Nearly complete mammalian skeletons, such as those of *Sinodelphys* and *Eomaia*, offer evidence for the ancestral skeletal adaptations of crown therians. The eight mammalian species discovered from the Yixian Formation have revealed a broad range of locomotory adaptations within the Yixian mammalian community (*48*). Body mass ranges from 45 to 70 g for zhangheotheriids (*7*) to ~20 to 25 g for the eutriconodont *Jeholodens* (*8*) and the multituberculate *Sinobaatar* (*11*). The eutherian *Eomaia* (*10*) and the metatherian *Sinodelphys* are 25 to 40 g. Only two gobiconodontids are much larger (200 and 3000 g, respectively) (*9*). *Jeholodens*, *Sinobaatar*, zhangheotheriids, and gobiconodontids show terrestrial adaptations by phalangeal proportions, profile of the claws, and other skeletal features. By contrast, the more derived *Sinodelphys* and *Eomaia* of the therian crown group have evolved scansorial adaptations in different ways, even though they are within the same small body size range (25 to 50 g) as several other obligatory terrestrial and coexistent mammalian taxa. The diversification of the earliest metatherians and eutherians appears to be associated with evolution of scansorial adaptations that may have facilitated the spread of these derived clades into more niches than were accessible to the terrestrial stem lineages of Mesozoic mammals.

References and Notes

1. M. C. McKenna, S. K. Bell, *Classification of Mammals Above the Species Level* (Columbia Univ. Press, New York, 1997).
2. Z. Kielan-Jaworowska, R. L. Cifelli, Z.-X. Luo, *Mammals from the Age of Dinosaurs: Origins, Evolution and Structure* (Columbia Univ. Press, New York, in press).
3. G. W. Rougier, J. R. Wible, M. J. Novacek, *Nature* **396**, 459 (1998).
4. Z.-X. Luo, R. L. Cifelli, Z. Kielan-Jaworowska, *Nature* **409**, 53 (2001).
5. Z.-X. Luo, Z. Kielan-Jaworowska, R. L. Cifelli, *Acta Palaeontol. Pol.* **47**, 1 (2002).
6. Etymology: *Sino* (Latin), China; *delphys* (Greek), uterus, commonly used suffix for marsupial taxa; *szalayi*, in honor of F. S. Szalay for his studies of metatherian evolution. Systematics: Class Mammalia, Subclass Metatheria, Order and Family incertae sedis. Holotype: CAGS00-IG03 (Fig. 1; Chinese Academy of Geological Sciences, Institute of Geology), an incomplete, flattened skeleton with some preserved soft tissues, such as costal cartilages and fur, on a shale slab; parts of hindlimb, pes, and shoulder girdle preserved on fragments of a counterslab. Locality and age: lacustrine beds of the Yixian Formation at the Dawangzhangzi Locality, Lingyuan County, Liaoning, China. The locality is correlated with the main fossiliferous horizon of the Yixian at the Sihetun site that was dated as 124.6 Ma (*12*) in the lower Barremian stage of the Lower Cretaceous.
7. Y.-M. Hu, Y.-Q. Wang, Z.-X. Luo, C.-K. Li, *Nature* **390**, 137 (1997).
8. Q. Ji, Z.-X. Luo, S.-A. Ji, *Nature* **398**, 326 (1999).
9. Y.-Q. Wang, Y.-M. Hu, J. Meng, C.-K. Li, *Science* **294**, 357 (2001).
10. Q. Ji *et al.*, *Nature* **416**, 816 (2002).
11. Y.-M. Hu, Y.-Q. Wang, *Chin. Sci. Bull.* **47**, 933 (2002).
12. C. C. Swisher, Y.-Q. Wang, X.-L. Wang, X. Xu, Y. Wang, *Nature* **398**, 58 (1999).
13. Diagnosis: Upper I4, C1, P4, M4; lower i4, c1, p4, m3 (Fig. 1). *Sinodelphys szalayi* differs from most mammaliaforms (*2*), eutriconodonts (*8, 9*), and multituberculates (*2, 11*) in having triangulated molar cusps; differs from zhangheotheriids and all pretribsophenic mammals in having a tricuspate talonid basin; differs from all known eutherians in having compressed, lanceolate posterior incisors, four (instead of three) upper molars, and apomorphies of the ankle and wrist; and differs from all known metatherians in dental formula. For full differential diagnosis, see (*14*).
14. For an expanded diagnosis, identification of skeletal structure, character list, taxa/character matrix, and results of phylogenetic analyses, see supporting data on *Science* Online.
15. Z. Kielan-Jaworowska, D. Dashzeveg, *Zool. Scr.* **18**, 347 (1989).
16. D. Sigogneau-Russell, D. Dashzeveg, D. E. Russell, *Zool. Scr.* **21**, 205 (1992).
17. R. L. Cifelli, *Nature* **401**, 363 (1999).
18. F. S. Szalay, *Evolutionary History of the Marsupials and an Analysis of Osteological Characters* (Cambridge Univ. Press, Cambridge, 1994).
19. L. G. Marshall, C. de Muizon, D. Sigogneau-Russell, *Mem. Mus. Natl. Hist. Nat.* **165**, 1 (1995).
20. M. S. Springer, J. A. W. Kirsch, J. A. Case, in *Molecular Evolution and Adaptive Radiation,* T. J. Givnish, K. J. Sytsma, Eds. (Cambridge Univ. Press, Cambridge, 1997), pp. 129–161.
21. C. de Muizon, *Geodiversitas* **20**, 19 (1998).
22. I. Horovitz, M. Sánchez-Villagra, *Cladistics* **19**, 181 (2003).
23. O. A. Reig, J. A. W. Kirsch, L. G. Marshall, in *Possums and Opossums: Studies in Evolution*, M. Archer, Ed. (Surrey Beatty, Sydney, Australia, 1987), pp. 1–89.
24. C. de Muizon, R. L. Cifelli, R. Céspedes, *Nature* **389**, 486 (1997).
25. M. J. Novacek *et al.*, *Nature* **389**, 483 (1997).
26. J. D. Archibald, A. O. Averianov, E. G. Ekdale, *Nature* **414**, 62 (2001).
27. G. W. Rougier, thesis, Universidad Nacional de Buenos Aires (1993).
28. F. S. Szalay, B. A. Trofimov, *J. Vertebr. Paleontol.* **16**, 474 (1996).
29. R. L. Cifelli, C. de Muizon, *J. Mamm. Evol.* **4**, 241 (1997).
30. A. O. Averianov, Z. Kielan-Jaworowska, *Acta Palaeontol. Pol.* **44**, 71 (1999).
31. Z. Kielan-Jaworowska, R. L. Cifelli, *Acta Palaeontol. Pol.* **46**, 377 (2001).
32. Z. Kielan-Jaworowska, *Palaeontol. Pol.* **33**, 103 (1975).
33. R. L. Cifelli, in *Mammal Phylogeny,* F. S. Szalay, M. J. Novacek, M. C. McKenna, Eds. (Springer-Verlag, New York, 1993), vol. 1, pp. 205–215.
34. W. A. Clemens, *Univ. Calif. Publ. Geol. Sci.* **62**, 1 (1966).
35. M. Sánchez-Villagra, K. K. Smith, *J. Mamm. Evol.* **4**, 119 (1997).
36. Z. Kielan-Jaworowska, *Palaeontol. Pol.* **38**, 5 (1978).
37. I. Horovitz, *J. Vertebr. Paleontol.* **20**, 547 (2000).
38. C. Argot, *J. Morphol.* **247**, 51 (2001).
39. F. S. Szalay, E. J. Sargis, *Geodiversitas* **23**, 139 (2001).
40. T. H. Rich *et al.*, *Rec. Queen Vic. Mus.* **106**, 1 (1999).
41. J. A. Lillegraven, *Annu. Rev. Ecol. Syst.* **5**, 263 (1974).
42. J. A. Lillegraven, *Univ. Tenn. Stud. Geol.* **8**, 1 (1984).
43. C. H. Tyndale-Biscoe, M. B. Renfree, *Reproductive Physiology of Marsupials* (Cambridge Univ. Press, Cambridge, 1987).

Downloaded from www.sciencemag.org on January 2, 2007

44. M. S. Springer, *J. Mamm. Evol.* **4**, 285 (1997).
45. C. Argot, *J. Morphol.* **248**, 76 (2002).
46. R. L. Cifelli *et al.*, *Nature* **379**, 715 (1996).
47. K. C. Beard, in *Primates and Their Relatives in Phylogenetic Perspective*, R. D. E. MacPhee, Ed. (Plenum, New York, 1992), pp. 63–90.
48. A. Weil, *Nature* **416**, 798 (2002).
49. D. L. Swofford *PAUP*–Phylogenetic Analysis Using Parsimony (*and other Methods)*, version 4.0b (Sinauer, Sunderland, MA, 2000).
50. We thank K. C. Beard, R. L. Cifelli, M. R. Dawson, Z. Kielan-Jaworowska, J. A. Lillegraven, M. J. Novacek, G. W. Rougier, and M. Sánchez-Villagra for many discussions that are relevant to this research; R. L. Cifelli and M. R. Dawson for improving the paper; A. Henrici and A. R. Tabrum for preparation; and M. Klingler for illustration of Fig. 1. Supported by NSF (USA) (Z.-X.L. and J.R.W.), the Ministries of Land Resources and Science and Technology of the People's Republic of China (Q.J.), NSFC (China) and the National Geographic Society (Z.-X.L.), and the Carnegie Museum of Natural History (Z.-X.L. and J.R.W.).

Supporting Online Material
www.sciencemag.org/cgi/content/full/302/5652/1934/DC1
SOM Text
Figs. S1 and S2
Matrix table (character distribution)
References
PAUP analysis

22 August 2003; accepted 10 November 2003

REPORTS

Subkelvin Cooling NO Molecules via "Billiard-like" Collisions with Argon

Michael S. Elioff,[1] James J. Valentini,[2] David W. Chandler[1]

We report the cooling of nitric oxide using a single collision between an argon atom and a molecule of NO. We have produced significant numbers (10^8 to 10^9 molecules per cubic centimeter per quantum state) of translationally cold NO molecules in a specific quantum state with an upper-limit root mean square laboratory velocity of 15 plus or minus 1 meters per second, corresponding to a 406 plus or minus 23 millikelvin upper limit of temperature, in a crossed molecular beam apparatus. The technique, which relies on a kinematic collapse of the velocity distributions of the molecular beams for the scattering events that produce cold molecules, is general and independent of the energy of the colliding partner.

The development of methods for the preparation and confinement of ultra-cold atoms, with temperatures in the 1 μK to 1 nK range (*1*), have made possible the generation of Bose-Einstein condensates (*2*–*4*), the observation of atom optics (*5*), the investigation of collisions at ultra-low energy (*6*), and the optical clock (*7*). Ultra-cold atom samples are prepared in a two-step process. Radiation pressure cooling of atoms, via laser light absorption, yields samples at <1 mK, at which temperature the atoms can be held in a magneto-optical or similar trap and the temperature further reduced by optical (*8*, *9*) or evaporative cooling (*10*).

The preparation and trapping of molecules at similar temperatures has been much desired, although not yet accomplished in a general way (*11*–*13*). The radiation pressure cooling that is used as the initial step in the trapping of ultra-cold atoms does not work well for molecules because of their more complex energy-level structure. Other methods for slowing or cooling have been demonstrated to accomplish the first step and produce molecules cold enough to be trapped and further cooled. The term "cooling" is reserved for processes that compress the velocity distribution by slowing the particles with higher velocities more efficiently than they slow particles with lower velocities. This process increases the phase space density of the molecules.

Cold molecule production processes include photoassociation of ultra-cold atoms (*14*–*17*); adiabatic tuning of a Feshbach resonance in a cold atomic gas (*18*, *19*); and buffer gas loading (*20*, *21*), which uses laser ablation (or molecular beam loading) of a gas into a cold He buffer gas cell wherein bulk collisions cool the molecules in an anti-Helmholtz magnetic trap equilibrated at ~1 K. Additionally, varying inhomogeneous electric fields in time has been used to slow molecules (*22*). In particular, Stark deceleration (*23*) can slow dipolar molecules to a stop when they have the appropriate Stark behavior. Another technique that has been proposed for slowing molecules is a spinning molecular beam source in which the velocity of the spinning source cancels the velocity of the molecules flowing through it (*24*). Although successful, each approach has limitations in applicability or execution.

We report here a cooling process for molecules that relies upon a single collision between the molecule and an atom in a crossed molecular beam apparatus that produces molecules with a laboratory velocity that is nominally zero. The technique relies on a kinematic collapse of the laboratory velocity distribution of molecules that are scattered with a particular recoil velocity vector in the center-of-mass (COM) frame. The method depends on the fact that in binary collisions, one of the collision partners can have a final COM-frame velocity that is essentially equal in magnitude and opposite in direction to the velocity of the COM, thus yielding a laboratory-frame velocity that is nearly zero. Cooling occurs because the COM velocity scales with initial NO velocity almost the same as does the recoil velocity.

Only collisions that result in NO molecules recoiling opposite to the direction of the motion of the COM experience the kinematic collapse. NO molecules recoiling in other directions have much larger laboratory velocities and quickly leave the scattering center. Thus, only the NO molecules that have had their velocity distribution narrowed by collision remain. This cooling process is not only general, but it is also realizable under easily accessible experimental conditions in crossed atomic and molecular beams.

The method does not rely on any particular physical property of either colliding species, because zero velocity is a consequence of the experimentally selectable energy and momenta of the collision pair. Moreover, this technique can be used to prepare a single, selectable ro-vibronic quantum state for trapping. We demonstrate this technique using inelastic collisions between NO molecules in one beam and Ar in the other, specifically $NO(^2\Pi_{1/2}, j = 0.5) + Ar \rightarrow NO(^2\Pi_{1/2}, j' = 7.5) + Ar$. Using an existing crossed molecular beam experimental apparatus that is not specifically optimized for the production of cold molecules, we generate scattered $NO(^2\Pi_{1/2}, j' = 7.5)$ with a velocity distribution that is centered about zero, with an upper limit root mean square (RMS) velocity of

[1]Combustion Research Facility, Sandia National Laboratories, Livermore, CA 94550, USA. [2]Department of Chemistry, Columbia University, New York, NY 10027, USA.

Downloaded from www.sciencemag.org on January 2, 2007